Supporting Information

The preparation route and final form of V-MXenes override the effect of the O/F ratio on their magnetic properties

Pavla Eliášová[a*], Břetislav Šmíd[b], Jana Vejpravová[b], Shuo Li[a], Federico Brivio[a], Michal Mazur[a], Daniel N. Rainer[a], M. Infas H. Mohideen[a], Russell E. Morris[c], Petr Nachtigall[a]

Computational methods

All calculations were performed at the density functional theory (DFT) level using the Vienna "*ab-initio*" simulation package (VASP)[1,2] and the Perdew–Burke–Ernzerhof (PBE) exchange–correlation functional[3]. The semi-empirical DFT-D3 method[4] was used to treat van der Waals interactions. Furthermore, the DFT+U method[5] was applied to assess the correct magnetic order of strongly correlated systems containing transition metals. A Hubbard correction of U = 3 eV was employed based on our previous study.[6] The Brillouin zone was represented by a special Monkhorst–Pack k-point mesh of 21 × 21 × 7, 21 × 21 × 1, 11 × 11 × 1 and 5 × 5 × 1 points for geometric and electronic structures of the MAX phase and unit cell, (2 × 2) supercell, and (3 × 3) supercell of MXenes, respectively. An energy cut-off of 500 eV was used to determine the self-consistent charge density for the plane wave basis sets. The structures were fully optimized until the maximum Hellmann–Feynman force on atoms was lower than 0.01 eV Å^{-1} and the total energy variation was lower than 1.0 ×10^{-5} eV. A vacuum (> 12 Å) was added in the direction perpendicular to the slab to model the isolated monolayers.

To evaluate the stability of functionalized $V_2CO_xF_{2-x}$ ($0 \le x \le 2$) MXenes, the formation energy (E_{form}) of the unit cell was calculated according to the following equation:

$$E_{form} = (E[V_2CO_xF_{2-x}] - E[V_2C] - \frac{x}{2}E[O_2] - \frac{2-x}{2}E[F_2])/2n \quad \text{(S1)}$$

where $E[V_2C]$ and $E[V_2CO_xF_{2-x}]$ stand for the total energies of pristine V_2C and functionalized $V_2CO_xF_{2-x}$ MXenes, respectively, $E[O_2]$ and $E[F_2]$ is the energy of O_2 and F_2 molecules in the gas phase, respectively, and n represents the ($n \times n$) supercell.

We used a scalar, collinear magnetic model, and we considered the ferromagnetic (FM) configuration and possible antiferromagnetic (AFM) states to calculate the preferred magnetic ground state structures of related MXenes (Figure S13). Assessing the full magnetic properties of these materials requires using a larger simulation scale that can be approached using the Ising model and to map the energy landscape to an effective classical spin Hamiltonian on a honeycomb lattice according to the following equation:

$$H_{spin} = \frac{1}{2}\sum_{i \neq j} J_{ij} S_i \cdot S_j$$

where S_i is the total spin magnetic moment of the atomic site i, J_{ij} are the exchange coupling parameters between two local spins, and the prefactor 1/2 accounts for the double counting of spin. We can extract the nearest-neighbor (J_1), second-nearest-neighbor (J_2), and third-nearest-neighbor (J_3) coupling constants from DFT calculations (for (2 × 2) $V_2CO_xF_{2-x}$ MXenes):

$$E_{AFM1} - E_{FM} = (3J_1 + 3J_3)S^2$$

$$E_{AFM3} - E_{AFM2} = (J_1 - 3J_3)S^2$$

$$E_{AFM2} - E_{AFM1} = (4J_2 - 2J_1)S^2$$

This approach enabled us to calculate the Curie temperature through Monte Carlo simulations performed with the open source software ALPS.[7]

Preparation of multilayered and delaminated V_2AlC films

Materials prepared by etching parent V_2AlC are denoted as multilayered V_2CT_x with an *ml-V_2CT_x* prefix. When using a mixture of concentrated acids (CA) HF (29M) and HCl (12M) for etching, we denote the sample with an additional prefix *CA*, i.e. *CA-ml-V_2CT_x*. Similarly, when using a mixture with diluted (DA) HCl acid (6M) and concentrated HF (29M), we denote the materials with the prefix *DA*, i.e. *DA-ml-V_2CT_x*.

Etching of the V_2AlC MAX phase

As shown in Figure S8, the PXRD pattern of V_2AlC powder (SEM image in Figure S10 mostly corresponds to the MAX phase with a (002) peak position at 13.5° 2θ[8]. In addition to this MAX phase, V_2AlC powder also contains other phases, such as vanadium oxides and aluminium oxide, as shown in the PXRD pattern (Figure S8). These phases can be formed during MAX phase synthesis. Their presence in minor fractions is usually not an issue as they can be dissolved during the etching treatment or separated during the delamination process.

Some authors have investigated suitable conditions for V_2AlC etching by comparing concentrated HF at RT for 72 hours with a mixture of concentrated HF + HCl at 50 ºC for 72 hours[9]. Under both conditions, multilayered V_2CT_x was formed, also containing an unreacted parent phase, but the treatment with a mixture of concentrated acids provided a higher yield. Similar conditions (concentrated HF + HCl at 40 ºC for 48 hours) were used in the latest paper to report a new synthetic approach for MXenes, more specifically V_2AlC[10]. In both studies, their parent MAX phase was prepared in their laboratory. By contrast, in this study, the MAX phase was purchased from a commercial vendor. Nevertheless, we started our experiments by reproducing their method, using a mixture of concentrated HF (29M) and HCl (12M) acids at 50 ºC.

Following the recommended safety procedures, we slowly added V_2AlC into a concentrated acid mixture, which was cooled in an ice bath. Despite our efforts, the procedure was not particularly

reproducible, though, as shown in Figure S9. The experiments in concentrated acids at 50 ºC yielded different multilayered V_2CT_x MXenes, as evidenced by the different positions of the (002) peak. In one case, transferring the reaction bottle into an oil bath preheated to 50 ºC even triggered an exothermic reaction, which released large bubbles of hydrogen, quickly turned the suspension green and even heated up the oil bath above 50º C. This reaction was stopped by cooling down in an ice bath. The PXRD pattern highlighted that the parent MAX phase was complete dissolved, leaving only Al_2O_3 and a mixture of vanadium oxides, as shown in Figure S9.

Based on these experiences, we continued the etching tests at room temperature to avoid unpredictable, exothermic reactions, thus developing a more reproducible method. Still, in most etching experiments with a concentrated acid mixture, we observed the formation of aluminium oxide. Even when the V_2AlC phase was meshed to the same particle size, as previously reported[9] (see SEM images in Figure S10), the quality of the starting material obviously varied, and therefore so did the etching conditions. But when diluting HCl to half (6M solution), we consistently obtained multilayered V_2CT_x with only a negligible or no fraction of Al_2O_3 and with a smaller portion of the unreacted MAX phase than with the concentrated acid mixture. In conclusion, the most efficient and reproducible etching conditions consist of applying a mixture of 29 M HF + 6M HCl to our commercially purchased V_2AlC MAX phase at room temperature for 72 hours.

Exfoliation of multilayered V_2CT_x

To exfoliate the layers, a freshly etched multilayered V_2CT_x (wet powder) was directly intercalated with a 25% tetramethylammonium hydroxide solution. Subsequent series of centrifugation and mechanical shaking yielded a black supernatant of exfoliated V_2CT_x layers. The exfoliated layers were had a bronze hue. To demonstrate the reproducibility of etching in a diluted acid solution, we prepared delaminated V_2CT_x, more specifically *DA-del-V_2CT_x (1)* and *DA-del-V_2CT_x (2)*, in two experiments to compare their properties. In their PXRD patterns (2), all films have the same profile with similar intensities, and the (002) peak has the same position at 6.9º 2θ (corresponding to d-spacing 1.28 nm). Only *DA-del-V_2CT_x (1)* shows low intensity peaks of the parent MAX phase, indicating a minor fraction of unreacted V_2AlC.

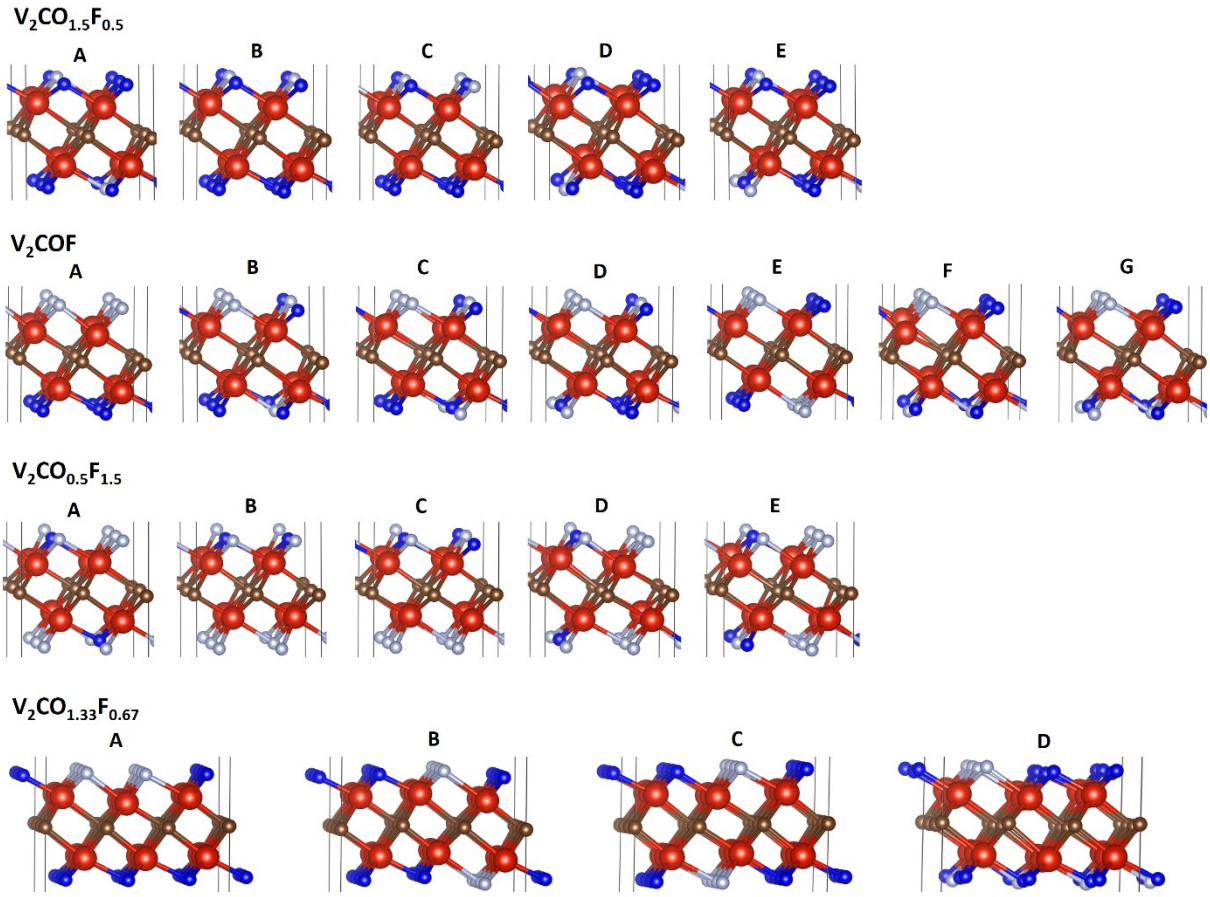

Fig.S1 The possible structures of $V_2CO_xF_{2-x}$ at different concentrations of x = 1.5, 1.0 and 0.5 in (2×2) supercell and x = 1.33 in (3×3) supercell. Red, brown, blue and gray balls represent V, C, O and F atoms.

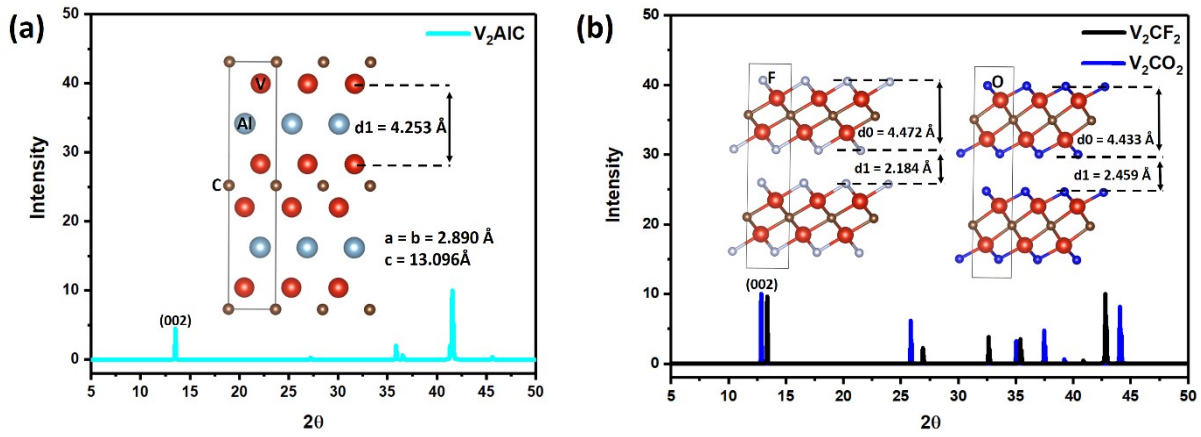

Fig.S2 Simulated PXRD of (a) the vanadium MAX phase and (b) stacking of V_2CO_2 and V_2CF_2 layers. The corresponding structures are shown in the insets. d_0 and d_1 stand for the thickness of the layer and the interlayer distance, respectively. Red, light blue, brown, blue and gray balls represent V, Al, C, O and F atoms.

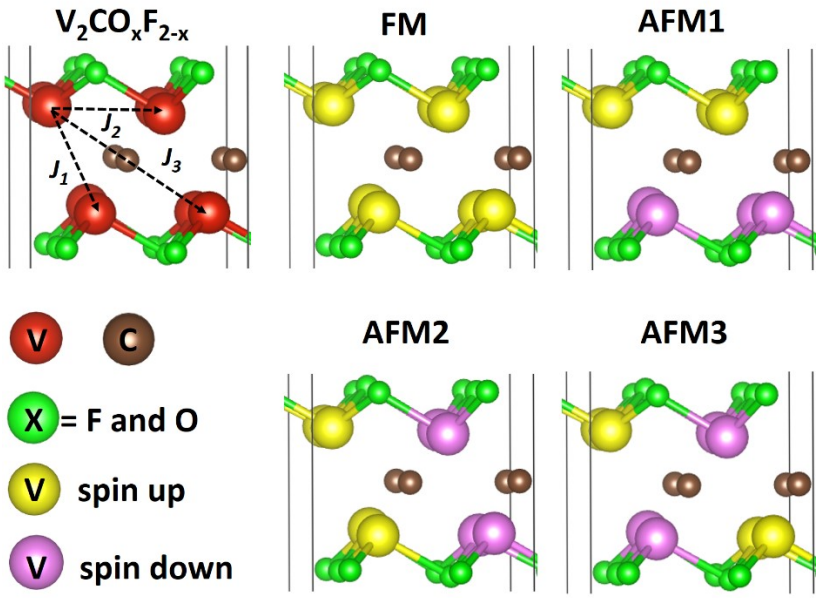

Fig.S3 Possible magnetic configurations of the $V_2CO_xF_{2-x}$ MXene and spin exchange parameters. Yellow and pink balls represent V atoms with spin up and spin down electron configurations.

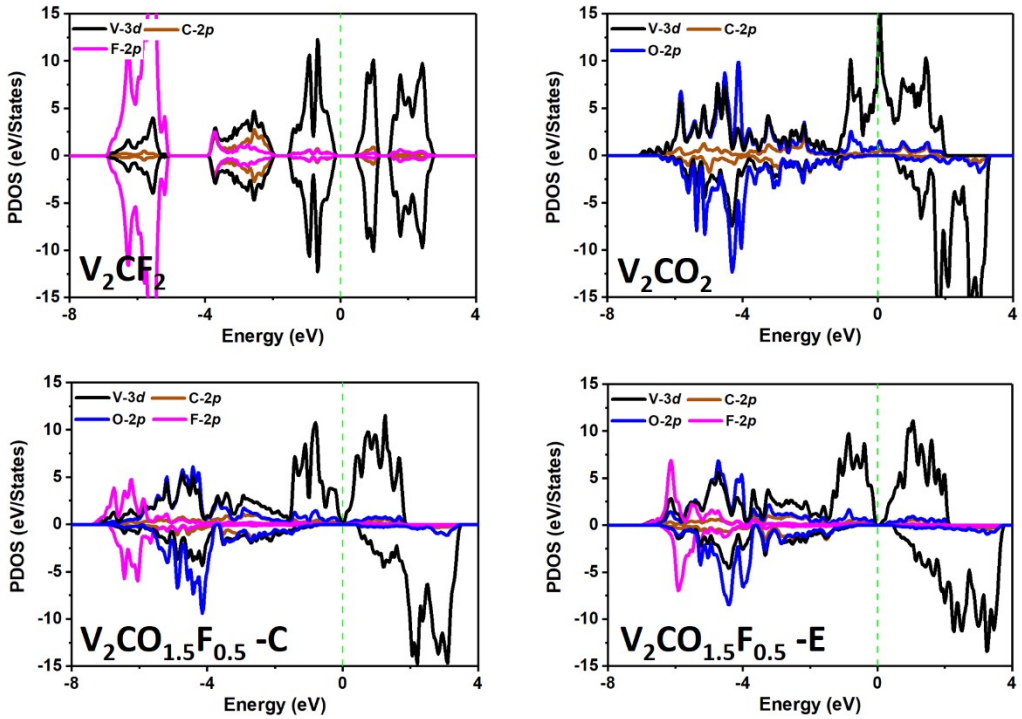

Fig.S4 Partial density of states (PDOS) of V-3d states and C, O and F-2p states for V_2CF_2, V_2CO_2 and $V_2CO_xF_{2-x}$-X MXenes in (2×2) supercell. -X stands for the specific configuration of the surface functional group, as defined in Fig. S1.

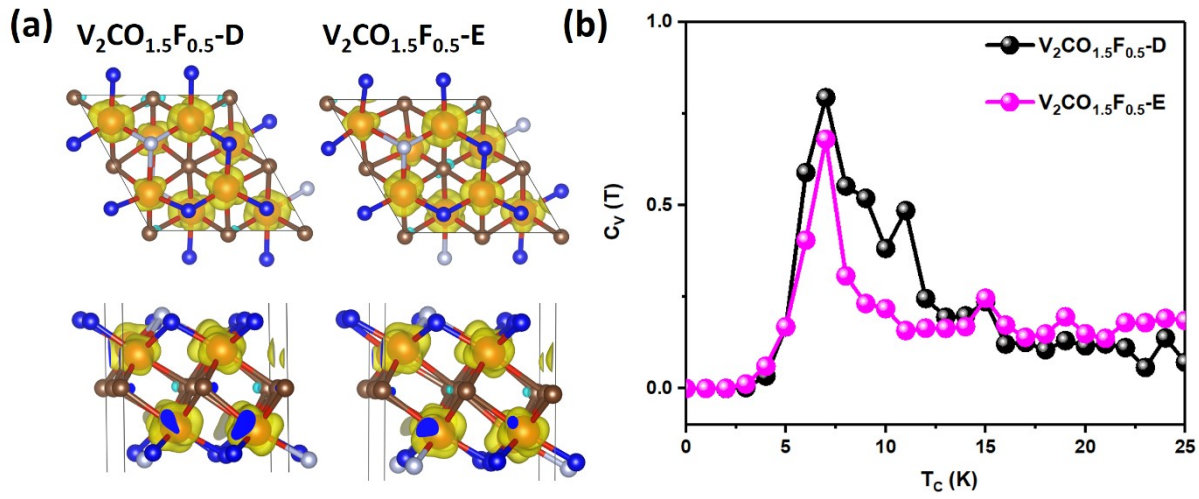

Fig.S5 (a) Spin-charge-polarized densities (SCD) and (b) simulated specific heat (C_V) as a function of temperature (T_C) for $V_2CO_{1.5}F_{0.5}$-D and $V_2CO_{1.5}F_{0.5}$-E. The isosurface of SCD is 0.03 e/Bohr^3. Red, brown, blue and gray balls represent V, C, O and F atoms.

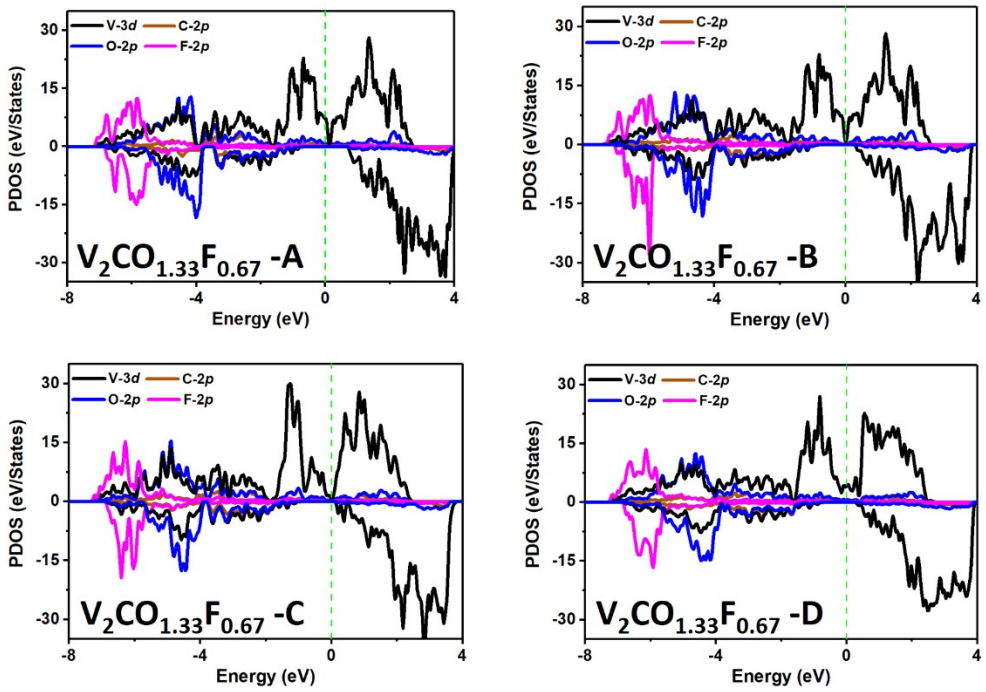

Fig.S6 Partial density of states (PDOS) of V-3d states and C, O and F-2p states for $V_2CO_{1.33}F_{0.67}$-X MXenes in (3×3) supercell. -X stands for the specific configuration of the surface functional group, as defined in Fig. S1.

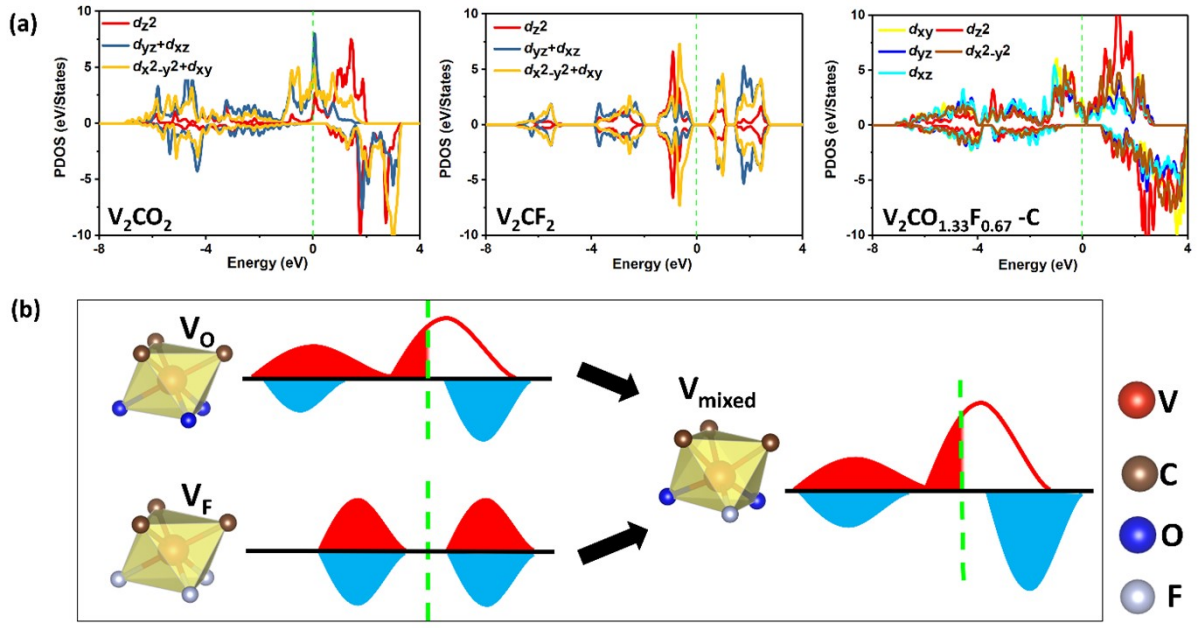

Fig.S7 (a) PDOS of V-3d orbitals of V_2CO_2, V_2CF_2 and $V_2CO_{1.33}F_{0.67}$-A MXenes. (b) Schematic diagrams of the V spin polarizations in symmetrically and asymmetrically functionalized surfaces. V_{mixed} represents the V atom in $V_2CO_{1.33}F_{0.67}$ MXenes.

Table S1 Calculated geometric parameters and electronic and magnetic properties. L is the lattice constant (in Å), E_{form} is the formation energy (in eV) of the unit cell, M is the average value of the magnetic moment of V atoms (in μ_B), Q is the average value of the charge of V atoms (in e) assessed by Bader charge analysis, G.S. is the magnetic ground state, and T_C/T_N is the Curie/Néel temperature (in K).

MXenes		L	E_{form}	M	Q	G.S.	T_C/T_N
V_2CO_2		2.95	-4.13	1.12	-2.15	FM	12
V_2CF_2		3.16	-4.89	2.10	-1.93	AFM2	38
$V_2CO_{1.5}F_{0.5}$	A	3.03	-4.42	1.44	-2.09	FM	34
	B	3.04	-4.42	1.39	-2.11	FM	32
	C	3.04	-4.42	1.39	-2.11	FM	48
	D	2.99	-4.45	1.39	-2.09	FM	7
	E	3.03	-4.45	1.39	-2.09	FM	7
V_2COF	A	3.09	-4.60	1.61	-2.05	FM	48
	B	3.06	-4.62	1.51	-2.04	AFM2	40
	C	3.08	-4.61	1.64	-2.04	FM	44
	D	3.10	-4.63	1.62	-2.06	FM	9
	E	3.08	-4.60	1.64	-2.04	FM	15
	F	3.08	-4.62	1.63	-2.05	FM	25
	G	3.06	-4.62	1.52	-2.04	AFM2	10
$V_2CO_{0.5}F_{1.5}$	A	3.13	-4.77	1.75	-2.00	AFM3	20
	B	3.09	-4.80	1.84	-1.98	FM	19
	C	3.13	-4.79	1.76	-1.99	AFM3	22
	D	3.10	-4.82	1.70	-2.00	AFM2	24
	E	3.14	-4.84	1.74	-2.00	AFM2	33
$V_2CO_{1.33}F_{0.67}$	A	2.99	-4.48	1.48	-2.09	FM	/
	B	2.99	-4.49	1.48	-2.08	FM	/
	C	2.98	-4.52	1.47	-2.10	FM	/
	D	3.02	-4.50	1.48	-2.08	FM	/

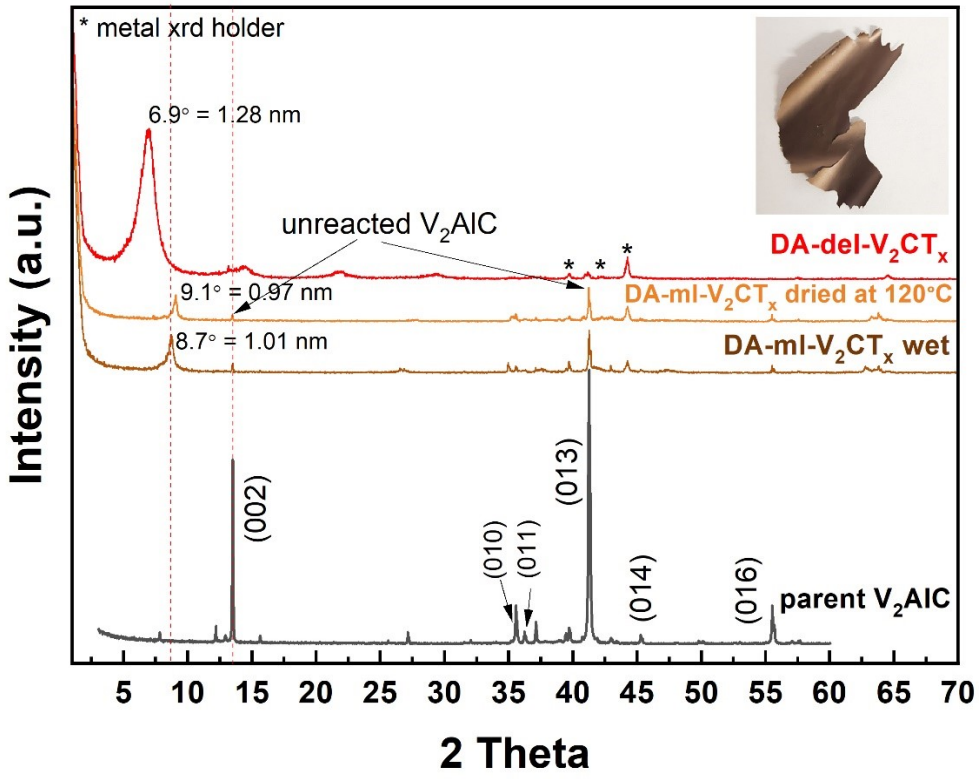

Fig.S8 X-ray powder (PXRD) pattern of the parent V_2AlC MAX phase and daughter MXenes after etching in diluted acid solution, DA-ml-V_2CT_x (1). The multilayered DA-ml-V_2CT_x (1) was measured directly after etching (designated as wet) and after drying at 120°C. After exfoliation and filtration of the colloidal suspension, the material is designated as DA-del-V_2CT_x (1). Additional peaks labeled with an asterisk are assigned to the metal XRD sample holder. The optical image of the shiny thin film of DA-del-V_2CT_x (1) is shown on the right upper corner.

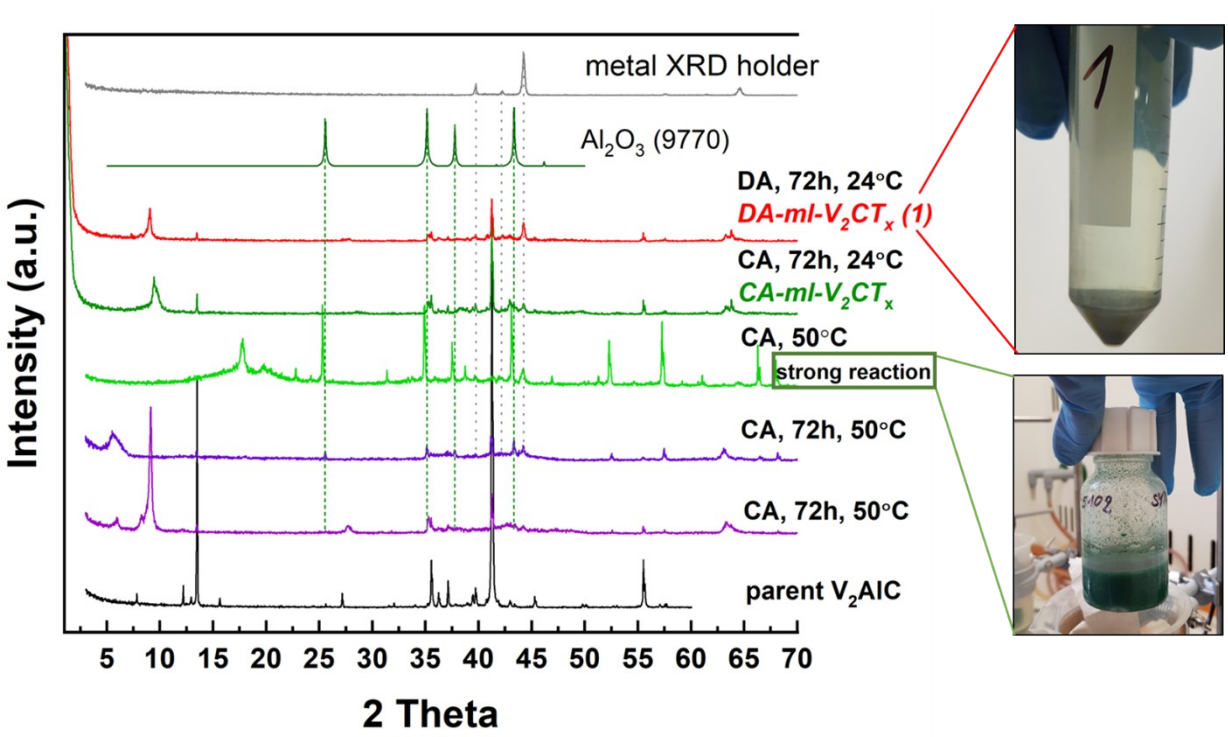

Fig.S9 Comparison of powder XRD patterns of the parent V_2AlC and daughter MXene materials prepared under different etching conditions. In some cases, the reflections of the metal XRD holders (stainless steel) are visible in the diffractograms of the materials. Photographs of the resulting etching solution are shown for two set of conditions – after the very strong, exothermic reaction and after the controlled reactions under milder conditions.

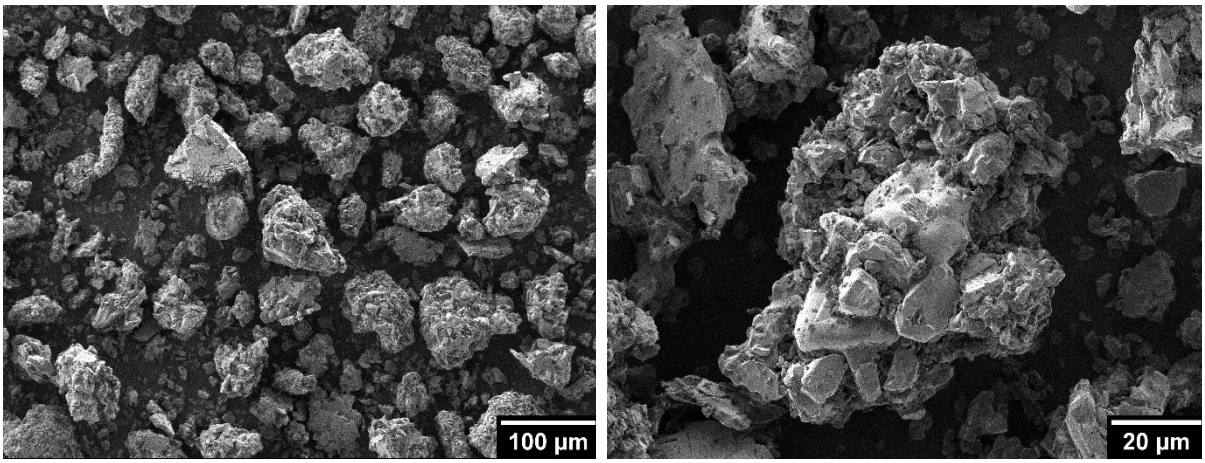

Fig.S10 Scanning electron microscopy images of a parent V_2AlC material.

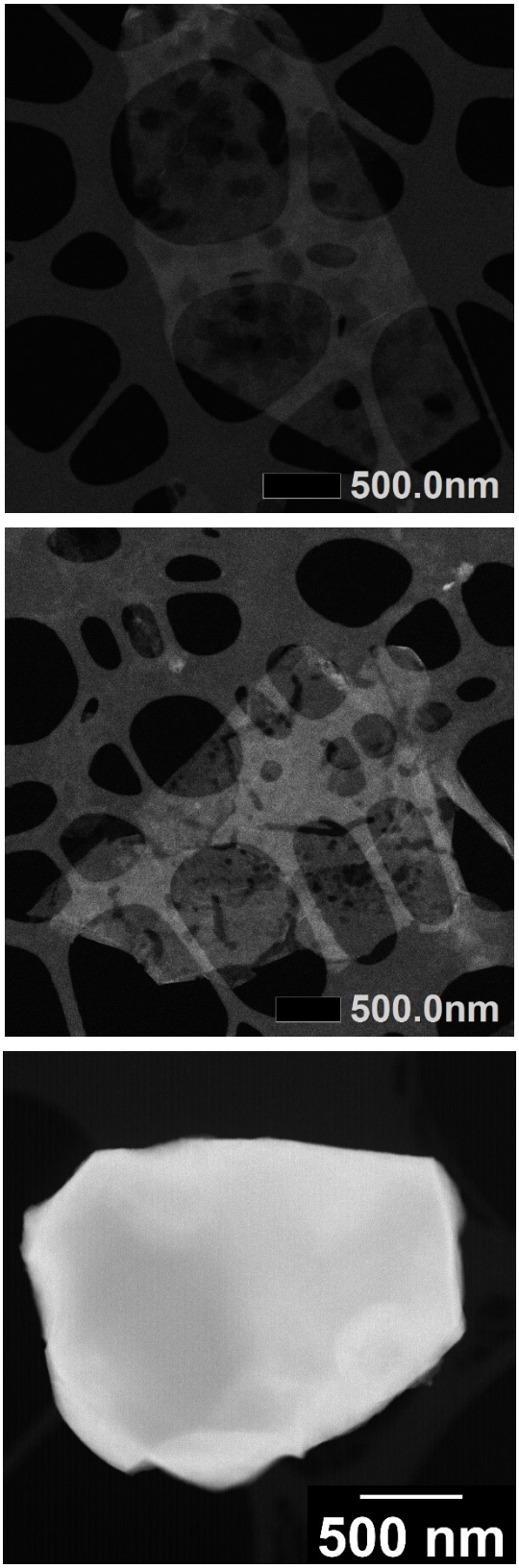

Figure S11 Scanning transmission electron microscopy images of DA-del-V_2CTx (1) (top two images) analyzed directly from the suspension of delaminated V_2CT_x and DA-ml-V_2CT_x (bottom image) analyzed in the form of powder.

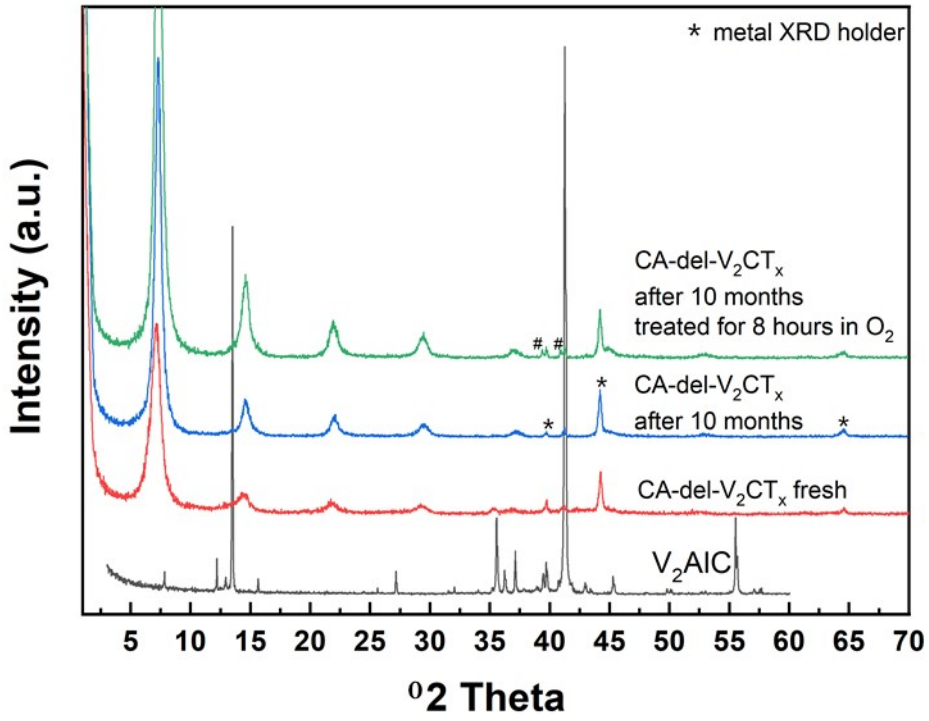

Fig S12: X-ray powder (PXRD) pattern of a parent V_2AlC MAX phase, freshly prepared CA-del-V_2CT_x film, the same film after 10 months of storage in a desiccator, and the same old film after 8 hours of treatment with oxygen flow. Two peaks of the unknown phase are labeled with # and do not correspond to any V_2O_5 or Al_2O_3 phase.

Table S2 Fitting results of XPS spectra from all V_2CTx materials prepared in this study.

		DA-ml-V_2CT_x		**DA-del-V_2CT_x (1)**		**DA-del-V_2CT_x (2)**		**CA-del-V_2CT_x**		**DA-del-4O_2-V_2CT_x**		**DA-del-8O_2-V_2CT_x**		**CA-del-8O_2-V_2CT_x**	
Region	*Name*	*Position*	*At. Conc.*	*Position*	*At. Conc.*	*Position*	*At. Conc.*	*Position*	*At. Conc.*	*Position*	*At. Conc.*	*Position*	*At. Conc.*	*Position*	*At. Conc.*
F 1s	V-F	684.68	9.01	684.66	7.23	684.63	8.23	684.72	10.49	684.49	4.88	684.51	5.37	684.51	3.48
V 2p	V (+2)	513.48	4.45	513.54	3.09	513.49	3.57	513.49	4.34	513.41	2.44	513.41	2.50	513.41	1.78
	V (+3)	514.62	10.39	514.62	6.14	514.62	7.55	514.62	9.05	514.62	4.46	514.62	4.34	514.62	3.18
	V (+4)	516.40	3.99	516.40	4.49	516.40	4.37	516.40	4.40	516.40	4.24	516.40	4.53	516.40	3.08
	V (+5)	517.80	2.99	517.80	2.06	517.80	2.10	517.80	2.25	517.80	1.78	517.80	1.89	517.80	1.78
O 1s	O-V	529.68	8.47	529.77	6.97	529.72	8.27	529.62	6.81	529.79	7.80	529.73	6.14	529.79	6.97
	H2O	531.37	10.94	531.39	12.14	531.30	7.39	531.06	9.74	531.20	10.35	531.20	14.48	531.20	8.99
	O-C/Si	532.88	6.77	532.48	8.26	532.70	8.17	532.39	5.49	532.35	12.26	532.35	8.34	532.35	15.10
C 1s	C-C	284.84	18.67	285.08	28.81	285.03	28.22	284.90	24.98	285.05	25.91	285.05	24.98	285.01	30.20
	V-C	282.00	8.01	282.40	4.88	282.38	5.33	282.40	5.80	282.21	4.09	282.23	4.02	282.25	2.87
	C-O	286.31	11.45	286.36	11.47	286.30	12.05	286.08	13.69	286.30	14.21	286.42	15.83	286.30	13.70
	C=O	288.45	2.49	288.40	1.75	288.45	2.32	288.40	0.14	288.17	4.21	288.10	4.33	287.98	5.48

Table S3 Results of the analysis using the modified Curie-Weiss law. C (m^3K/mol) – Curie constant, θ_P – paramagnetic Curie temperature, μ_{eff} – effective magnetic moment, χ_0 – Pauli susceptibility.

Material	**C (m^3K/mol)**	**θ_P (K)**	**μ_{eff} (μ_B)**	**χ_0 (m^3/mol)**
V_2AlC	$<1\times10^{-9}$	-	-	9.3×10^{-8}
DA-ml-V_2CT_x	4.4×10^{-6}	1.7	1.67	2.5×10^{-8}
DA-del-V_2CT_x (1)	4.8×10^{-7}	0.9	0.55	2.9×10^{-8}
CA-del-V_2CT_x	4.9×10^{-7}	0.9	0.56	6.5×10^{-9}
DA-del-4O_2-V_2CT_x	5.8×10^{-7}	2.0	0.61	5.5×10^{-9}
CA-del-8O_2-V_2CT_x	5.8×10^{-7}	1.6	0.61	2.3×10^{-9}

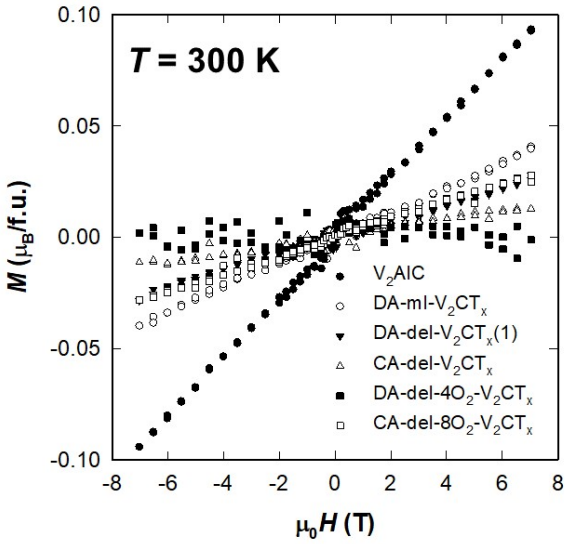

Figure S13 Magnetization isotherms recorded at 300 K.

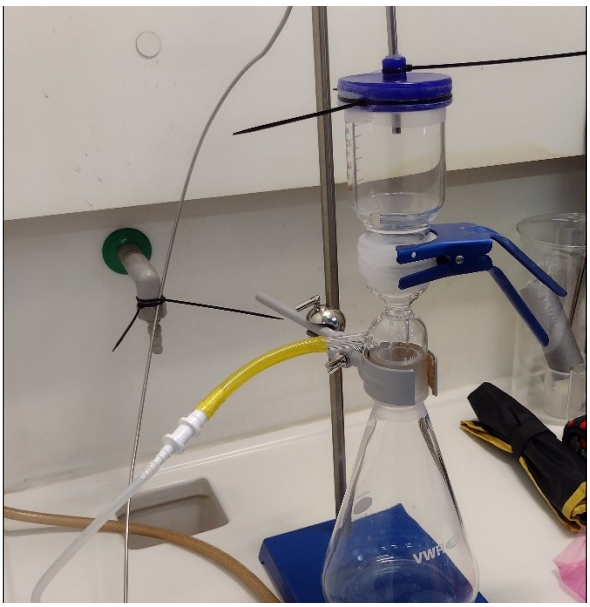

Fig.S14 Home-made apparatus for oxygen treatment involving filtration set with a solid frit bed. The flow was controlled at the output from the aperture.

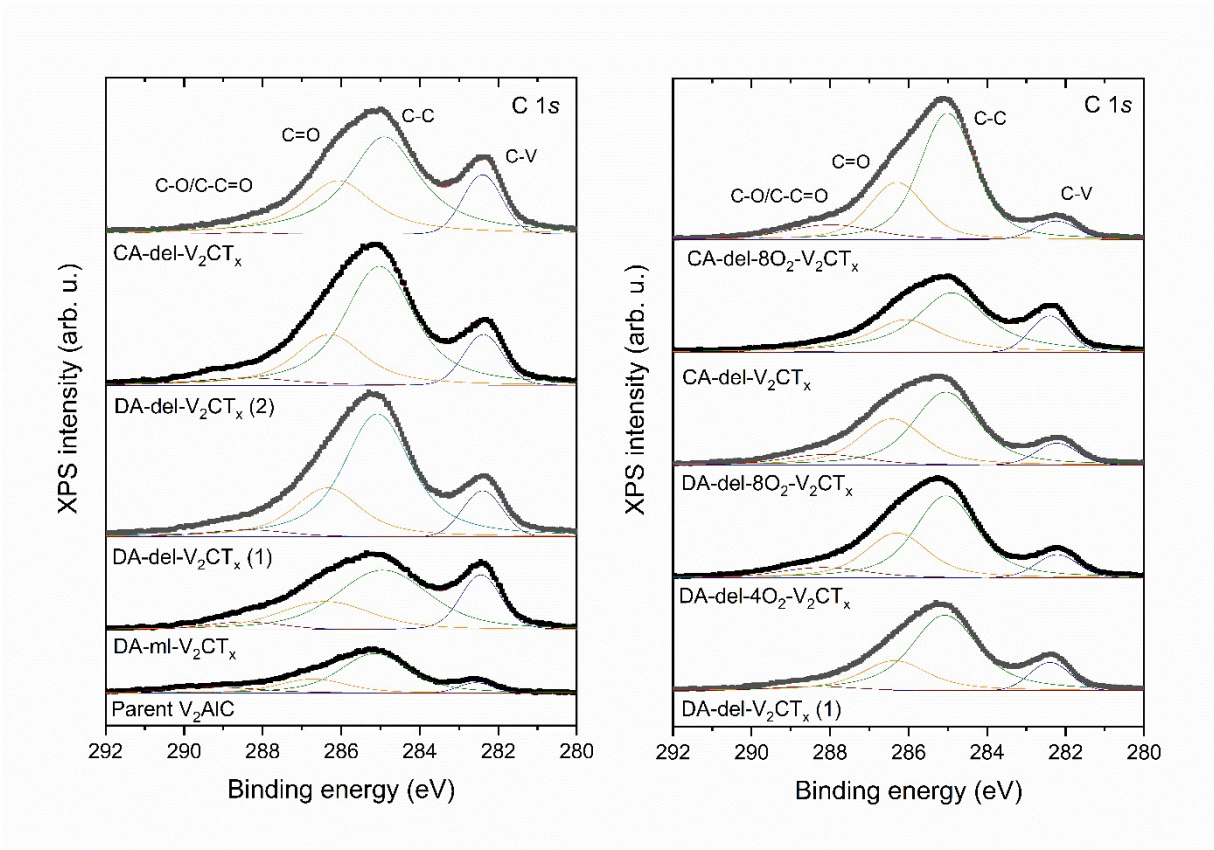

Fig.S15 XPS spectra of C 1*s* taken from parent V_2AlC, multilayered DA-ml-V_2CTx, and all delaminated films V_2CT_x. Complementary data to Figure 4 in the main text.

Reference

1. Kresse, G. and J. Hafner, *Ab initio.* Physical Review B, 1993. **47**(1): p. 558-561.
2. Kresse, G. and D. Joubert, *From ultrasoft pseudopotentials to the projector augmented-wave method.* Physical Review B, 1999. **59**(3): p. 1758-1775.
3. Perdew, J.P., K. Burke, and M. Ernzerhof, *Generalized Gradient Approximation Made Simple.* Physical Review Letters, 1996. **77**(18): p. 3865-3868.
4. Grimme, S., et al., *A consistent and accurate ab initio parametrization of density functional dispersion correction (DFT-D) for the 94 elements H-Pu.* The Journal of Chemical Physics, 2010. **132**(15): p. 154104.
5. Dudarev, S.L., et al., *Electron-energy-loss spectra and the structural stability of nickel oxide: An LSDA+U study.* Physical Review B, 1998. **57**(3): p. 1505-1509.
6. He, J., P. Lyu, and P. Nachtigall, *New two-dimensional Mn-based MXenes with room-temperature ferromagnetism and half-metallicity.* Journal of Materials Chemistry C, 2016. **4**(47): p. 11143-11149.
7. Albuquerque, A.F., et al., *The ALPS project release 1.3: Open-source software for strongly correlated systems.* Journal of Magnetism and Magnetic Materials, 2007. **310**(2, Part 2): p. 1187-1193.
8. M. Shekhirev, C. E. Shuck, A. Sarycheva and Y. Gogotsi, *Progress in Materials Science*, 2021, **120**, 100757.
9. K. Matthews, T. Zhang, C. E. Shuck, A. VahidMohammadi and Y. Gogotsi, *Chem. Mat.*, 2022, **34**, 499-509.
10. S. Vorotilo, C. E. Shuck, M. Anayee, M. Shekhirev, K. Matthews, R. W. Lord, R. Wang, I. Roslyk, V. Balitskiy, V. Zahorodna, O. Gogotsi and Y. Gogotsi, Graphene and 2D Materials, 2023, DOI: 10.1007/s41127-023-00059-1.